COMPDYN 2015
5th ECCOMAS Thematic Conference on
Computational Methods in Structural Dynamics and Earthquake Engineering
M. Papadrakakis, V. Papadopoulos, V. Plevris (eds.)
Crete Island, Greece, 25–27 May 2015

ADAPTIVE CONTROL OF THE ROCKING MOTION OF ART OBJECTS

Rosario Ceravolo [1], Marica L. Pecorelli [1], and Luca Zanotti Fragonara[1]

[1] Politecnico di Torino
Corso Duca degli Abruzzi, 24 -10129 Torino, Italy
{rosario.ceravolo,marica.pecorelli,luca.zanottifragonara}@polito.it

Keywords: Art objects, Rocking, Adaptive control, Non-linear response system.

Abstract. *The seismic behaviour of many art objects and obelisks can be analysed in the context of the seismic response of rigid blocks. Starting from the pioneering works by Housner (1963), a large number of analytical studies of the rigid block dynamics were proposed. In fact, despite its apparent simplicity, the motion of a rigid block involves a number of complex dynamic phenomena such as impacts, sliding, uplift and geometric nonlinearities. Methods that prevent the possible overturning were also presented in the past years, especially to protect statues and art objects with respect to seismic events. In the more general context of control, to date a current strategy is represented by base isolation.*

In this paper a novel adaptive control strategy for protecting monolithic art objects was investigated. The control under study follows a feedback-feedforward scheme that is realised by adjusting the stiffness of anchorages with adaptive stiffness located at the two corners of the block. A numerical comparison was made between the behaviour of the unanchored block, the anchored block with a system having constant stiffness and the anchored block with adaptive stiffness. Finally, numerical investigations were carried out in order to verify the expected efficiency of the proposed control system, and to validate simple control laws.

1 INTRODUCTION

Many studies and codes are devoted to the seismic protection of existing buildings and in particular of museum buildings. On the other hand, the protection of the contents of museums, e.g. art objects on display or kept in storage, has received much less attention by earthquake engineering standards. In fact, the protection of museum collections against seismic hazard is increasingly attracting interest among the governments and the scientists, since their damage could irreparably affect the cultural heritage worldwide.

The past and recent seismic events have clearly shown the high vulnerability of art objects and of museum contents even in case of moderate earthquakes. Indeed, the art objects in many museums are displayed in a way that does not ensure stability during a seismic event. The storage areas are often overloaded without any consideration for the seismic risk. The seismic mitigation of art objects requires a multidisciplinary approach in order to find a compromise between safety and conservation. In addition, the objects on display need to take into account the issues of aesthetic enjoyment of artefacts as well as constraints related to space.

From a structural point of view, the seismic behaviour of art objects in many cases can be analysed within the context of the dynamic response of rigid blocks. The literature counts a large number of analytical studies on the non-linear dynamics of the rigid block, starting from the pioneering work by Housner in 1963 [1]. The motion of rigid blocks on a rigid plane, can be classified into six types: rest, slide, rotation, slide-rotation, translation jump and rotation jump. The equations of motions, transition of motions and motions after the impact between the block and the floor, in the presence of horizontal and vertical accelerations, was investigated by Ishiyama in 1982 [2]. Depending on the form and magnitude of the excitation [2-3] and on the geometry and mass distribution of the objects, the artefacts can experience all the types of motion mentioned above. Among different cases, a particular and fundamental role is covered by the rocking motion, that cause objects to fall from their supports or to collide with other objects.

To mitigate the damage due to rocking motion and limit the probability of overturning, four different strategies are currently used [4]. They consist of lowering the centre of gravity of the artefacts, adjusting the base-to-height ratio proportions of the art objects, fixing the objects to the floor/wall or separating the objects from the ground using base isolation devices. The efficacy of the first two strategies is strictly connected with the dynamics of rigid block motion. During the rocking motion of a rigid block the restoring force is originated by its own rotational inertia. Lowering the centre of gravity of the artefact allows increasing the restoring force of the system and consequently its stability. The second strategy, adjusting the base-to-height ratio proportions, can be easily explained with regard to the effect of slenderness on overturning, studied for the first time by Housner [1] and investigated subsequently by several authors [5-6]. These two strategies, as well as anchoring the objects to the ground, must be used carefully because by moving the objects together with the ground, the amount of forces transmitted to the artefact can be very high. In this case, the art object is forced to bend and deform, instead of oscillating rigidly around the two corners, so an accurate evaluation of the stress level is required. To avoid mechanical failure of the artefacts indeed the mechanical limit of the material must not be reached during the entire seismic event. Stress failure occurring at the area of load concentration or at the area of material weakness is highly likely.

In contrast to the significant amount of basic analytical theoretical research on the response of stand-alone rocking structures, there are relatively few theoretical studies on the response of structures retrofitted against rocking. The seismic isolation of rocking objects was considered in several recent works concerning the behaviour of the anchored blocks [7-8]. In particular Dimentberg et al. [9] investigated the behaviour of an anchored block excited by white

noise, while Makris et al. [10] studied its response to pulse-type ground motions. Makris et al. showed that there is a finite frequency range where the conclusions drawn by Dimentberg et al. [9] do not hold. The study demonstrates that for most of the loading frequency range anchored blocks survive higher acceleration than free-standing blocks. However, there is a frequency range where the opposite happens.

Most retrofitting strategies to avoid toppling of structures that exhibit rocking behaviour during earthquakes consist in preventing this type of motion instead of limiting it or controlling it. The aim of this paper is to allow rocking motion as a means of seismic isolation, and to use a control strategy to enhance its performances. Rocking as a seismic isolation technique is currently proposed for bridges [11] and building [12]. Starting from the idea that a controlled rocking motion, far from the overturning condition, can be a good way to reduce the vulnerability and the stress transmitted to the artefacts, a deformable anchorage, with constant and adaptive stiffness, is examined in this paper. Using the example of Michelangelo's San Matteo sculpture allocated in the "Galleria dei Prigioni" in Florence, whose dynamics has been studied by other authors [13], this paper investigates the behaviour of the free-standing block and the anchored block utilising springs having different stiffness.

2 MODEL OF THE BLOCK

The governing equations of rocking motion of unanchored (Figure 1a) and anchored (Figure 1b) rigid blocks received a special attention in the literature. Housner in [1] defined the governing equations of rocking motion of a rigid block subjected to horizontal and vertical base excitations, taking into account the nonlinear effects. These equations were then modified by Makris et al. [10] in order to consider the presence of unilateral restraints placed at the corners of the rigid block. A brief summary of the two dynamic models is reported hereinafter.

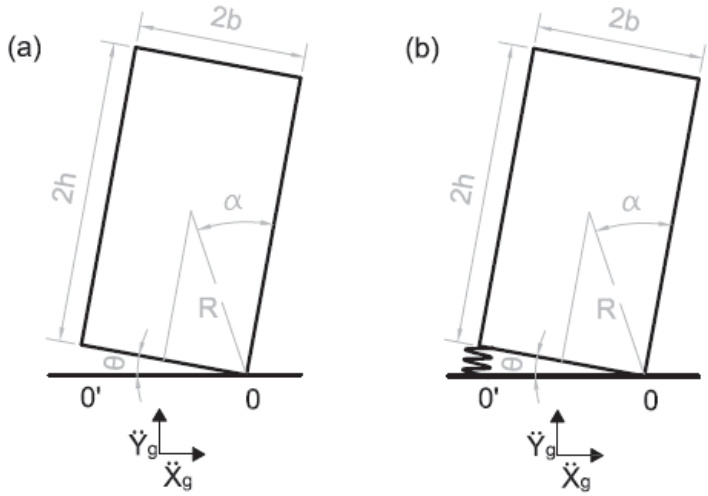

Figure 1: Idealization of the artefact as rigid rocking object, subjected to horizontal and vertical excitation (a) unanchored artefact (b) anchored artefact.

2.1 Initial response

Figure 1a and Figure 1b show an unanchored and anchored rigid block resting on horizontal rigid supporting base subjected to horizontal and vertical base excitations. The block remains at rest for small base excitations and starts to oscillate around the corner 0 or 0' when the base excitation increases and Equation (1) is satisfied:

$$\left|m\ddot{X}_g\right|h > b\, m\left(g + \ddot{Y}_g\right) \tag{1}$$

Three different types of motion may characterize the initial response of a rigid block: pure rocking, pure sliding and slide-rock motion [14-15]. In this work the coefficient of friction (μ_s) between the block and its base is assumed to be sufficiently large so that the object enters in a pure rocking motion without experiencing any sliding. Therefore, the coefficient of friction is assumed to satisfy the following conditions:

$$\left|m\ddot{X}_g\right| \leq \mu_s m\left(g + \ddot{Y}_g\right) \tag{2}$$

$$\frac{3\gamma g - 3\gamma\ddot{Y}_g + 4\ddot{X}_g + \gamma^2\ddot{X}_g}{3\gamma\ddot{X}_g + g + 4\gamma^2 g - \ddot{Y}_g - 4\gamma^2\ddot{Y}_g} \leq \mu_s \tag{3}$$

where: $g =$ the gravitational acceleration; $m =$ the mass of the block; $\mu_s =$ the coefficient of static friction; $\ddot{X}_g =$ horizontal base excitation; $\ddot{Y}_g =$ vertical base excitation; $\gamma = h/b$ is the slenderness of the block (see Figure 1).

2.2 Governing equations of the unanchored rigid block

The governing equation of motion for the rigid object with positive angular rotation can be derived by the rotational equilibrium about the corner 0:

$$I_0\ddot{\theta}(t) + mR\ddot{X}_g cos(\alpha - \theta) + m\left(g + \ddot{Y}_g\right)Rsin(\alpha - \theta) = 0 \tag{4}$$

where: $I_0 =$ moment of inertia of the block about 0; $R =$ the distance from 0 and the centre of mass of the block; $\alpha = cot^{-1}(h/b)$ is the critical angle beyond which the overturning will occur to the object under gravity alone. Similarly, the rocking about 0 is governed by the equation:

$$I_0\ddot{\theta}(t) + mR\ddot{X}_g cos(\alpha + \theta) - m\left(g + \ddot{Y}_g\right)Rsin(\alpha + \theta) = 0 \tag{5}$$

Introducing the frequency parameter of the rectangular block, defined as:

$$p = \sqrt{\frac{mgR}{I_0}} \tag{6}$$

the Equations (4) and (5) can be expressed in the compact form:

$$\ddot{\theta}(t) + p^2\left\{\left(1 + \frac{\ddot{Y}_g(t)}{g}\right)sin\left(sgn[\theta(t)]\alpha - \theta(t)\right) + \frac{\ddot{X}_g(t)}{g}cos\left(sgn[\theta(t)]\alpha - \theta(t)\right)\right\} = 0 \tag{7}$$

where $sgn[\ \ ]$ denotes the signum function.

An additional equation, connecting the angular velocities immediately before and after the impact, must couple with Equation (7), to derive the motion of a rigid block to a generic external excitation.

2.3 Governing equations of the anchored rigid block

In order to consider the presence of the unilateral anchorages at the two corners of the block (Figure 2), an additional term needs to be introduced in Equation (7). This term represents the resisting moment of the spring in tension and can be assumed to be:

$$M_{s,k} = K \cdot 4btan\left|\frac{\theta(t)}{2}\right| \cdot 2bcos\left|\frac{\theta(t)}{2}\right| = 8R^2 sin^2\alpha\, Ksin\left|\frac{\theta(t)}{2}\right| \quad (8)$$

where K = the stiffness of the anchorage.

By substituting Equation (8) into Equation (7) the rocking of the rectangular block will be described by:

$$\ddot{\theta}(t) + p^2\left\{\left(1 + \frac{\ddot{Y}_g(t)}{g}\right)sin\big(sgn[\theta(t)]\alpha - \theta(t)\big) + \frac{\ddot{X}_g(t)}{g}cos\big(sgn[\theta(t)]\alpha - \theta(t)\big) + \frac{M_{s,k}}{I_0 p^2}f_{L,1}(\theta)f_{L,2}(\theta) + \frac{M_{s,k}}{I_0 p^2}f_{R,1}(\theta)f_{R,2}(\theta)\right\} = 0 \quad (9)$$

where $f_{R,1}(\theta)$ and $f_{L,1}(\theta)$ are fracture functions for the right and the left springs, respectively, and are defined as:

$$f_{R,1}(\theta) = f_{L,1}(\theta) = \begin{cases} 1 & if \quad |\theta(t)| \le \theta_y \\ 0 & if \quad |\theta(t)| > \theta_y \end{cases} \quad (10)$$

where $f_{R,2}(\theta)$ and $f_{L,2}(\theta)$ are two functions used to establish which of the two springs is working during the rocking motion, and are defined as:

$$f_{R,2}(\theta) = \left(\frac{1 - sgn[\theta(t)]}{2}\right) \quad (11)$$

$$f_{L,2}(\theta) = \left(\frac{1 + sgn[\theta(t)]}{2}\right) \quad (12)$$

Equation (8) reflects a large displacement formulation, accounting for a spring elongation equal to $4b\ tan|\theta/2|$ and an eccentricity of $2b\ cos|\theta/2|$with respect to the rotation corner.

2.4 Impact energy dissipation

The angular velocity decreases when the angle of rotation reverses and the rotation centre swaps from points 0 to 0' and vice versa, due to energy loss during the impact. Housner [1] derived a model to calculate the angular velocity of the rigid body immediately after the impact and the energy dissipated during the impact. This model uses the following assumptions: (1) the impact is punctual; (2) the impact time t_I is very short; (3) the block remains at the same position during the impact time. Under these assumptions the relation between the two angular velocities, immediately before the $\dot{\theta}(t_I^-)$ and after the impact $\dot{\theta}(t_I^+)$ can be derived by means of the principle of conservation of the angular moments. Writing the momentum equation just before the impact and immediately after:

$$I_0\dot{\theta}(t_I^-) - m\dot{\theta}(t_I^-)2bRsin\alpha = I_0\dot{\theta}(t_I^+) \quad (13)$$

the following relationship between $\dot{\theta}(t_I^-)$ and $\dot{\theta}(t_I^+)$ is obtained for the rectangular block as:

$$e = \frac{\dot{\theta}(t_I^+)}{\dot{\theta}(t_I^-)} = 1 - \frac{2mR^2}{I_0}sin^2\alpha = 1 - \frac{3}{2}sin^2\alpha \quad (14)$$

In the literature e^2, or r, is referred to as "coefficient of restitution" and it is a measure of the energy dissipated at the impact. The value of e given by Equation (14) reflects the maximum value of the coefficient of restitution for a block with slenderness α under rocking motion. In this study, it is assumed that the coefficient of restitution fits exactly the value of Equation (14), even if in real practice additional energy is lost also due to interface mechanisms. Therefore the real value of the coefficient of restitution is generally smaller than e^2.

In order to evaluate whether after the impact the object will maintain a full contact with the base or will undergo uplift on the other corner, the overturning moment M_o and the resisting moment M_s should be compared. The object will rest if the following condition is satisfied:

$$|M_s| > |M_o| \tag{15}$$

2.5 Condition to sustain rocking motion

In order to avoid sliding during the entire duration of the rocking motion, the ratio between horizontal reaction $f_x(t)$ and vertical reaction $f_y(t)$ at the contact points between the block and the base, points 0 and 0' in Figure 1, must always satisfy the following condition:

$$\left|\frac{f_x(t)}{f_y(t)}\right| < \mu_s \tag{16}$$

The horizontal and vertical reactions at contact points 0 or 0' will fluctuate with time, and their value can be derived from the dynamic equilibrium in the horizontal and vertical directions:

$$f_x(t) = m\left[\ddot{X}_g(t) + \ddot{x}(t)\right] \tag{17}$$

$$f_y(t) = m\left[\ddot{Y}_g(t) + g + \ddot{z}(t)\right] \tag{18}$$

where $x(t)$ = horizontal displacement and $z(t)$ = vertical displacements of the centre of mass of the block.

2.6 Sources of nonlinearity

There are four different sources of nonlinearity in the equation of the rocking object described in Equation (7): the transition from one governing equation to the one at the instant of impact (when the centre of rotation changes from one edge to the other); the impact energy dissipation (which induces a jump discontinuity in the angular velocity); the geometric effect of the slenderness ratio of the object and last but not least the coupling of the vertical excitation with the rocking response.

These different sources of nonlinearity were investigated by several authors [16-17].

3 NUMERICAL ANALYSES

3.1 Geometry of the rigid block

Equation (7) is solved hereinafter referring to block dimensions that are of special interest for cultural heritage. More general conclusions would require the non-linear equation of motion to be solved for different values of parameter p. However, the results obtained for art objects, while being useful in themselves, may still support qualitative interpretations and extensions to more general sizes of blocks.

The geometric dimensions chosen for the block are: 2b = 0.60 m; 2h = 2.72 m, with a mass

of 3361 Kg, which matches the scale of the equivalent symmetric rectangular block of the Michelangelo's San Matteo sculpture [13]. The excitation applied to the block is always a one-sine pulse, which represents a typical choice in literature on rocking [1]. The sculpture object of the study is represented in Figure 2.

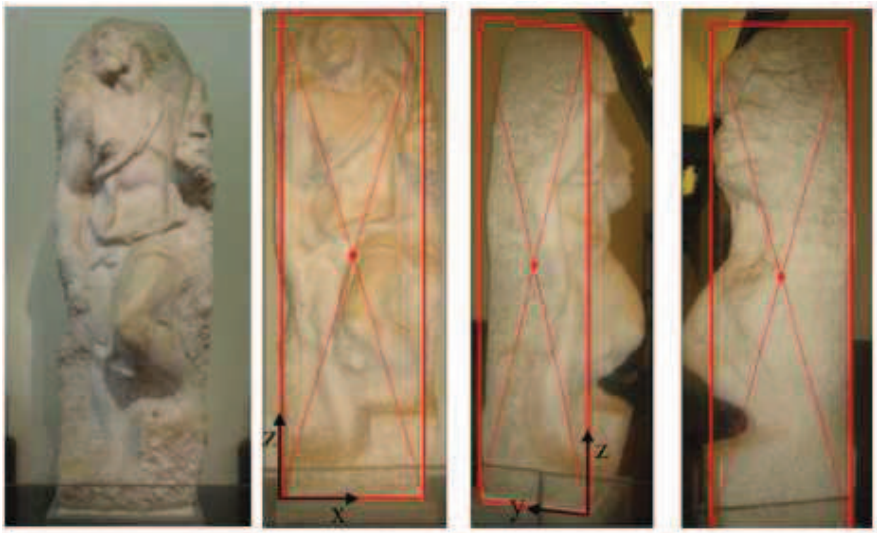

Figure 2: S. Matteo sculpture and equivalent rectangular block [13].

3.2 Numerical algorithm description

Closed form solutions for the rocking response to simple excitation forms are only found in the small displacement range. Therefore, the dynamic response of the rigid block subjected to one-sine pulses were determined numerically in Matlab ®, by integrating Equations (7) and (9) through a fourth-order Runge-Kutta scheme. The time-step used in the numerical integration was set to 0.0025 s [18]. Starting from the rest state of the rigid block, the actual corner of rotation, and therefore the reference equation to integrate, is determined from the sign of the horizontal base excitation. For positive value of $\ddot{X}_g(t_0)$, the block starts to rotate around the left corner (negative rotation), while for negative value it rotates around the right corner (positive rotation). The same equation is used for subsequent time steps until the sign of rotation θ changes. At each step, the condition $\theta_i \cdot \theta_{i+1} \geq 0$ is checked in order to establish the changes of rotation corner. If this condition is not satisfied, the velocity immediately before the impact, $\dot{\theta}(t_I^-)$, is evaluated and the velocity just after the impact, $\dot{\theta}(t_I^+)$, is determined by means the Equation (14). With the initial condition $\theta(t_I) = 0$ and $\dot{\theta}(t_I) = \dot{\theta}(t_I^+)$ the equation of motion on the other corner is used to evaluate the motion of the block in the subsequent time interval until the rotation angle θ will change its sign. The accuracy of the numerical procedure for the free-standing and for the anchored block has been validated for different types of base excitation. The response of the free-standing block under constant excitation, pulses and harmonic loadings were compared with the results found by Housner (linearized equations) [1], Makris et al. [19] and Spanos et al. [20], respectively. Similarly, the behaviour of the anchored block has been validated by implementing a numerical work of Markis et al.[10]. For instance, the S. Matteo equivalent rectangular block overturned when subjected to a constant acceleration of 0.2822g applied for 0.6380 s, but did not topple with a slightly shorter excitation, for example 0.6300 s (Figure 3), this being in agreement with Housner's formulas about overturning by constant acceleration [1].

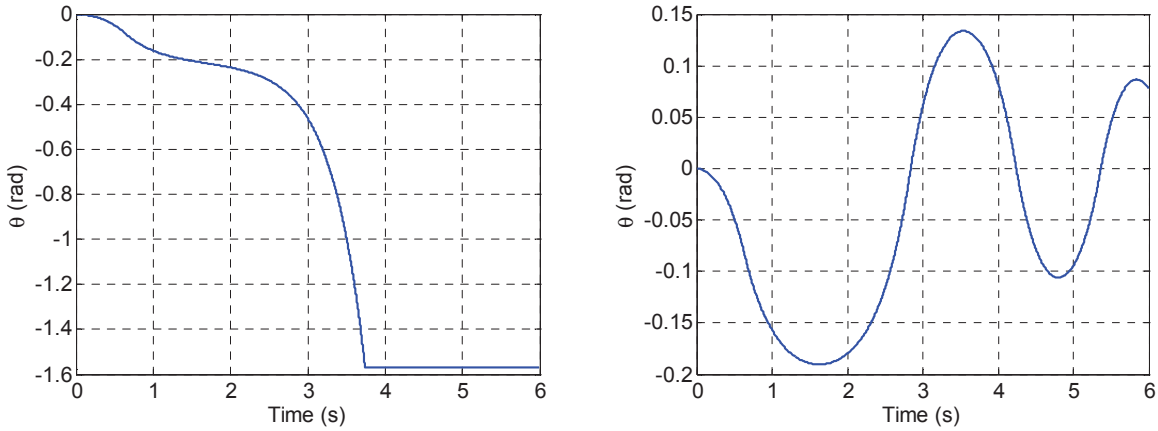

Figure 3: Linearized dynamic responses of S. Matteo equivalent rectangular rigid block subjected to a constant acceleration of 0.2822g applied for 0.6380s (left) and 0.6300 s (right).

3.3 S. Matteo block: free-standing conditions

The dynamic behaviour of S. Matteo equivalent rectangular block subjected to a generic base excitation cannot be established in advance, if not at a statistical level [5]. Indeed, the response of the system not only depends on the amplitude and frequency content of the excitation but also on its particular time-history. The same value of accelerations in a different succession can overturn the rigid block or not.

Aiming to improve the seismic behaviour of a rigid block, the response under one-sine pulse excitation is studied, characterized by different amplitudes a_{p0} and frequencies ω_p. Focusing on the dynamic response of the rigid block subjected to one-sine excitation constitutes the first step for controlling the dynamic behaviour of the block under a generic loading (e.g. earthquake).

In accordance with the studies conducted by Makris et al. [19], in the overturning spectra of the free-standing S. Matteo rectangular block (Figure 4) it is possible to distinguish between two overturning modes. The first mode occurs when there is an impact between the block and the floor before toppling, while in the second one the overturning occurs without any impact. In the frequency range examined in this study, overturning with impact, for a given value of ω_p/p, is typically observed for smaller amplitude of one-sine pulse, if compared with amplitudes that characterize overturning without impact.

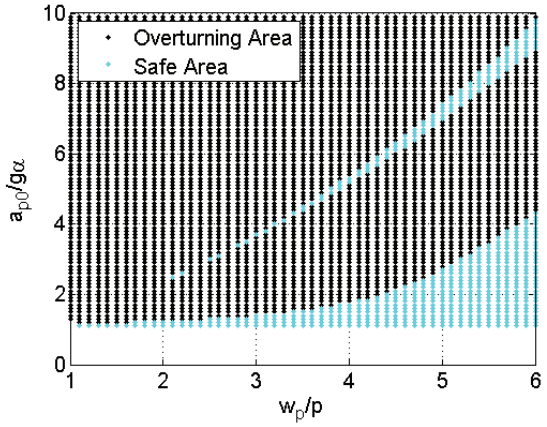

Figure 4: Overturning spectra of free-standing S. Matteo block ($p = 2.2985$) subjected to one-sine pulse.

3.4 S. Matteo block: anchored conditions with constant stiffness

The presence of anchorages provides additional resistance against toppling, compared to the free-standing block. Until the failure of the restrainers, indeed, the restoring force due to the self-weight of the block (see Figure 5) is supplemented by the restoring force engaged by the elastic-brittle anchorage in tension, as given in Equation (8).

In the following, the behaviour of the block anchored with restrainers, having different values of stiffness K, is determined and compared. K is chosen assuming that the failure of the restrainer occurs for a fix value of strength, but for different values of elongation. Failure strength is taken as equal to $0.4\,mg$ while the ultimate rotations are respectively α, $\alpha/2$, $\alpha/3$ and $\alpha/4$. The strength of the anchorage must be chosen as a function of the localized stress and the internal stress that the artefact is able to resist; in this study it was set in accordance with the work of Makris [10]. The first value of θ that brings the restrainers to failure is named θ_f, that corresponds to the angle α beyond which the overturning would occur for the object under gravity load alone. The other values examined were chosen as fractions of the first one. In Figure 6 the total restoring force is reported for the four types of anchorages under study.

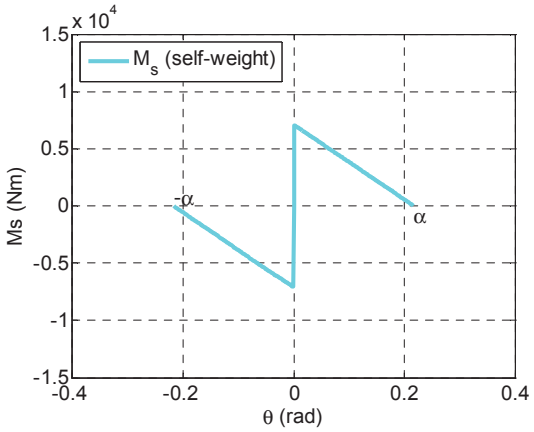

Figure 5: Restoring force due to self-weight.

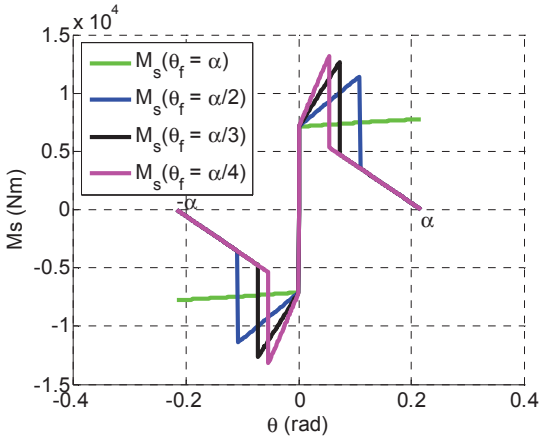

Figure 6: Total restoring force.

The basins of attraction of the rest state, i.e. $\theta = 0$, and of the overturning one, i.e. $\theta = |\pi/2|$, have been calculated for all the values considered for K (Figure 7). Each boundary of a basin of attraction has been determined by equating the total energy of the block at the generic time t to the potential one at the position $\theta = \alpha$ (corresponding to the minimum energy for block overturning). The equations of the boundary for each of the two overturning modes (without and with impact) read:

$$\dot{\theta}_1(t) = sgn[\alpha - \theta(t)]\, p \sqrt{2\big[1 - cos\big(\alpha - \theta(t)\big)\big] + \frac{b\,K}{2p^2 I_0}\left(tan\left|\frac{\alpha}{2}\right| - tan\left|\frac{\theta}{2}\right|\right)} \quad (19)$$

$$\dot{\theta}_1(t) = sgn[\alpha - \theta(t)]\, p \sqrt{2\left[\frac{1 - cos\alpha}{r}\right] + cos\alpha - cos(\alpha - |\theta|) + \frac{b\,K}{2p^2 I_0}\left(tan\left|\frac{\alpha}{2}\right| - tan\left|\frac{\theta}{2}\right|\right)} \quad (20)$$

Figure 7 reports the basins of attraction of S. Matteo block, for both the anchored and unanchored condition. It is worth noticing that in the range $-\alpha \leq \theta \leq \alpha$ the velocity required for the block to overturn increases with the stiffness of the restrainers.

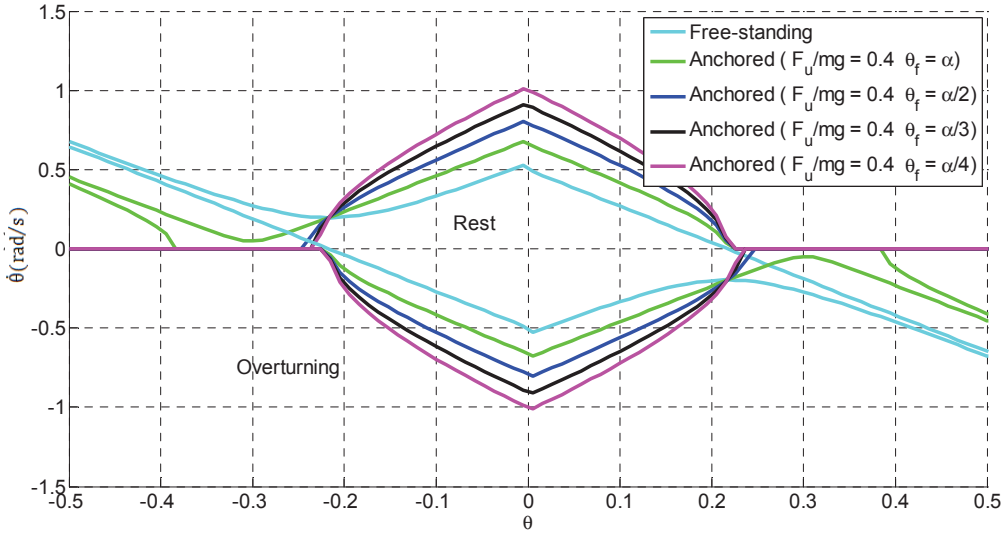

Figure 7: Basins of attraction in the state space for the investigated cases.

With a more rigid anchorage, an expansion of the basin of attraction of the rest state is observed in Figure 7. However, an increase of K does not imply a reduction of overturning risk for the block. In fact, the overturning spectra of the block (see Figures 8-11) reflect a more complex behaviour. The amplitude activating the second overturning mode (without any impact with the floor) is regardless from the stiffness of the anchorage. The value of K, instead, affects significantly the shape and the size of the overturning area associated to the overturning with impact mode. In that case, the amplitude requested, for a given value of ω_p, decreases or remains constant when increasing stiffness. This behaviour, which may seem counterintuitive, can be explained observing the dynamics of the system in the state space: the stiffness of the anchorage not only affects the basins of attraction, but it also influences the history of $(\theta, \dot{\theta})$, thus increasing the vulnerability of the object with respect to the second mode of overturning.

The different shape and size of overturning areas, as depending on the different connection to the floor, entails the possibility to select a value of stiffness that keeps the object within the safety domain. This can be realised when the one-sine pulse excitation is known both in terms of amplitude and frequency. In the next section, a strategy based on an adjustable anchorage is investigated to keep the system stable with respect to a measured excitation.

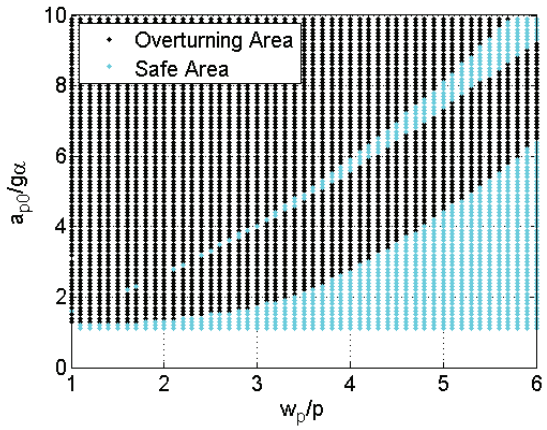

Figure 8: Overturning spectra of S. Matteo block

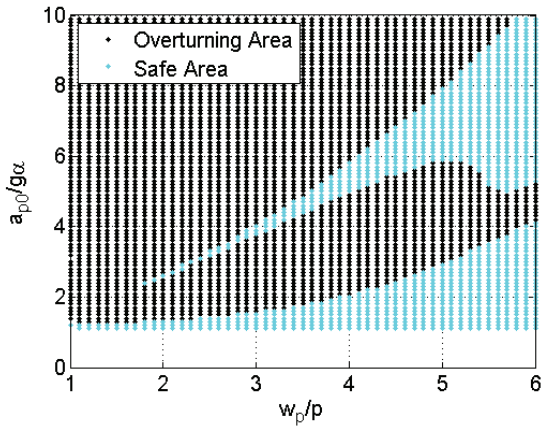

Figure 9: Overturning spectra of S. Matteo block

for $\theta_f = \alpha$ due to one-sine pulses.

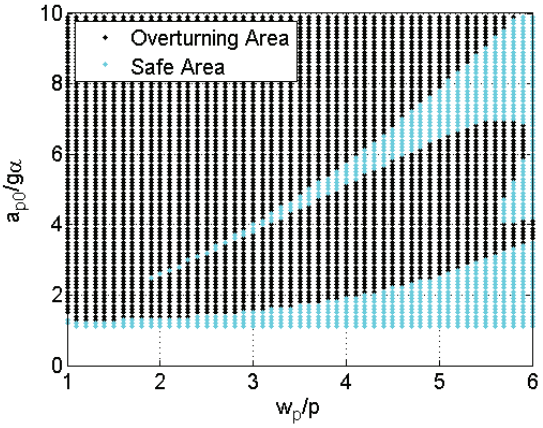

Figure 10: Overturning spectra of S. Matteo block for $\theta_f = \alpha/3$ due to one-sine pulses.

for $\theta_f = \alpha/2$ due to one-sine pulses.

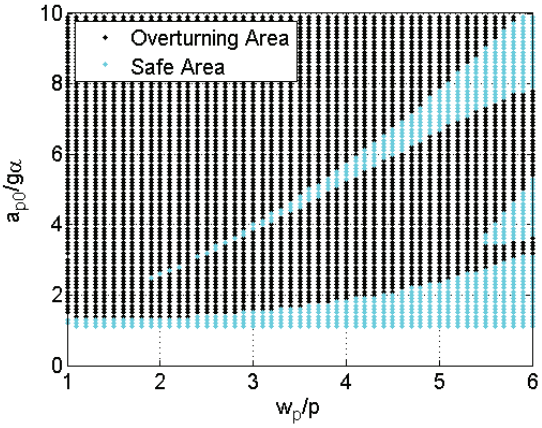

Figure 11: Overturning spectra of S. Matteo block for $\theta_f = \alpha/4$ due to one-sine pulses.

3.5 S. Matteo block: anchored conditions with adaptive stiffness

The performance of a control law applied to an adaptive anchorage is finally investigated. The stiffness of the anchorage/restrainer is assumed to switch between two fix values, K_{max} and K_{min}, as a function of the excitation and of the state of the rigid block. In order to evaluate the benefit of using an adaptive stiffness for the restrainer, the higher value of the stiffness, K_{max}, was chosen to correspond to the value of the less rigid spring examined in Section 3.4 $\left(F_u/mg = 0.4\ \theta_f = \alpha\right)$. Two different values, $K_{min} = 0.5\ K_{max}$ and $K_{min} = 0.1\ K_{max}$, were investigated.

Two different strategies are employed for setting the value of K at the generic time t. The first strategy consists in minimising the absolute value of the total work, and it applies when the block is excited. The second strategy, which applies in free oscillations conditions, consists in minimising the work done by the anchorage, this time in its signed value. Therefore, during the excitation, the stiffness is assigned using the following law:

$$K(t+1) = \begin{cases} K_{max} & if \quad -a_g(t)\cdot\theta(t) > 0 \\ K_{min} & if \quad +a_g(t)\cdot\theta(t) < 0 \end{cases} \tag{21}$$

Instead, during the free oscillations, the law to be used is:

$$K(t+1) = \begin{cases} K_{max} & if \quad |\theta(t)| - |\theta(t-1)| > 0 \\ K_{min} & if \quad |\theta(t)| - |\theta(t-1)| < 0 \end{cases} \tag{22}$$

The work done at time t by the excitation and by the unilateral anchorage can be written accordingly as follows:

$$W_p(t) = -m\ddot{X}_g R cos(\alpha - |\theta(t-1)|)\cdot[\theta(t) - \theta(t-1)] \tag{23}$$

$$W_a(t) = -8b^2 K sin\left|\frac{\theta}{2}\right|\cdot[\theta(t) - \theta(t-1)] \tag{24}$$

In Figures 12 and 13 the overturning spectra are reported for $K_{min} = 0.5\ K_{max}$ and $K_{min} = 0.1\ K_{max}$: the two diagrams show how reduced values of K_{min} can positively affect the response of the block (e.g., the overturning with impact disappears for $\omega_p/p > 3.7$). In particular, the use of an adjustable anchorage, adapted in accordance with Equations (21) and (22), improves the dynamic behaviour of the block independently of the characteristics of the

one-sine pulse excitation.

In order to show the performances of the control of the block in a sample excitation case ($w_p/p = 4$ $a_{p0}/\alpha g = 2.7$), Figures 14 and 15 compare on the time-histories of rotation angle and angular velocity of S. Matteo block, equipped with constant and adaptive anchorage ($K_{min} = 0.5\ K_{max}$), respectively. Correspondingly, Figure 16 depicts the normalised time-history of the values assumed by the stiffness of the adaptive anchorage in order to control the block. It is worth to highlight that the stiffness of the anchorage at the rotation pole in ineffective, thus in the plots it was assigned a zero value.

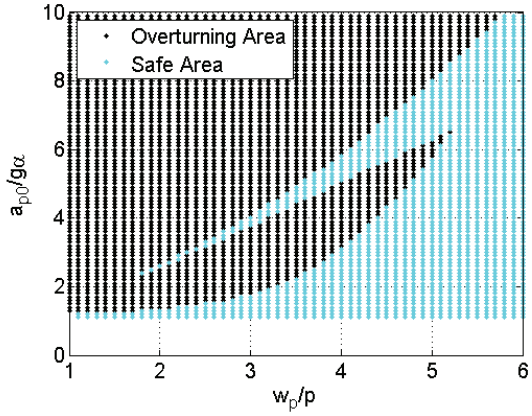

Figure 12: Overturning spectra for $K_{min} = 0.5\ K_{max}$.

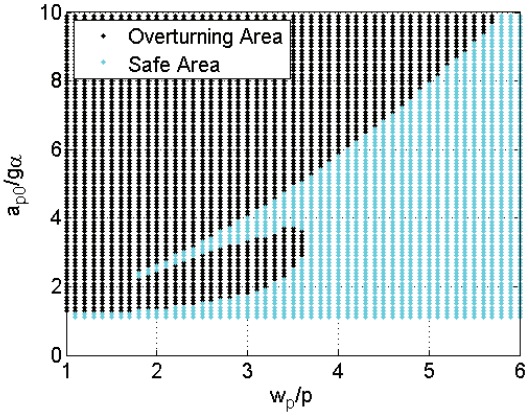

Figure 13: Overturning spectra for $K_{min} = 0.1\ K_{max}$.

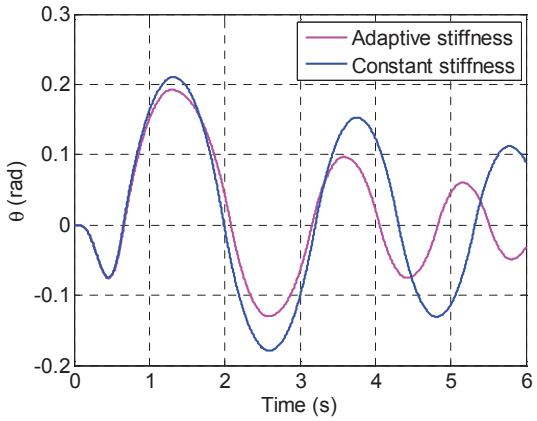

Figure 14: Time-history of the rotation angle for the S. Matteo block: with and without control.

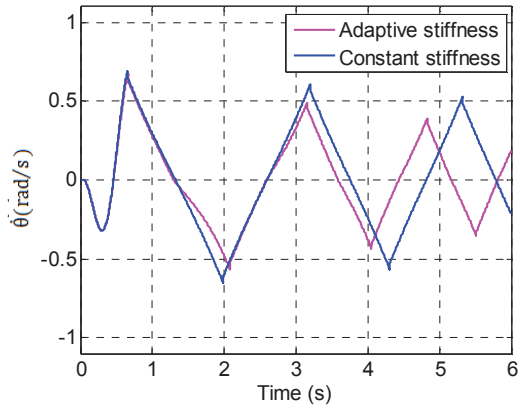

Figure 15: Time-history of the angular velocity for the S. Matteo block: with and without control.

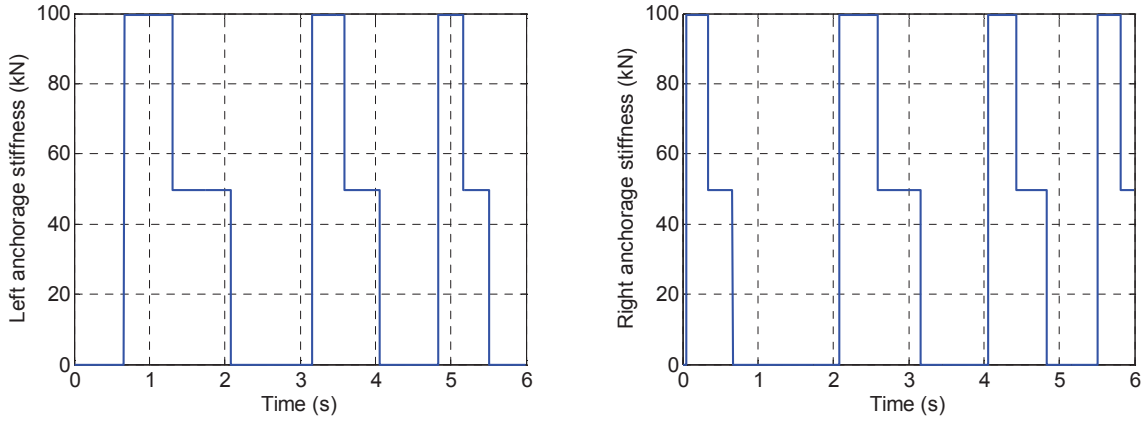

Figure 16: Time-history of the stiffness on the left and right corner of the block.

4 CONCLUSIONS

This paper examined a simple strategy for controlling the rocking response of art objects. The assumed control devices consist in adaptive unilateral restrainers connected to the ground, whose stiffness can be adjusted according to simple energetic laws. A few numerical investigations that regarded a famous statue located in the "Galleria dei Prigioni" in Florence were reported. At first, the overturning spectra, calculated for one-sine pulse excitations, of the statue were analysed with constant stiffness of restrainers. Such diagrams show that: (i) the first mode of overturning (with impact) is significantly affected by the characteristics of the anchorage; (ii) the second mode of overturning (without impact) is not influenced by the stiffness of the anchorage, since in this case the overturning of the block occurs for a fixed amplitude depending only on the loading frequency; (iii) the different shape and size of the overturning area of the same block with different connections suggests that an appropriate value of stiffness can actually prevent overturning of the block under one-sine pulse excitation.

In accordance with the previous observations, a strategy for adjusting the stiffness of the restrainers was proposed that minimise the total work done by the external excitation and by the anchorage system. The simulations performed on the statue showed that the first mode of overturning (with impact) can be appreciably reduced by such type of control. Thus a practical implementation of the presented control strategy can potentially reduce the vulnerability of artefacts that exhibit rigid block behaviour.

REFERENCES

[1] G.W. Housner, The behaviour of inverted pendulum structures during earthquakes. *Bulletin of the Seismological Society of America*, **53**, 403-417, 1963.

[2] Y. Ishiyama, Motion of rigid bodies and criteria for overturning by earthquake excitations. *Earthquake Engineering and Structural Dynamics*, **10**, 635-650, 1982.

[3] T. Taniguchi, Non-linear response analyses of rectangular rigid bodies subjected to horizontal and vertical ground motion. *Earthquake Engineering and Structural Dynamics*, **31**, 1481-1500, 2002.

[4] M. Lowry, B.J. Farrar, D. Armendariz, J. Podany, Protecting collection in the J. Paul Getty Museum from earthquake damage. *Western Association for Art Conservation (WAAC) Newsletter*, **29**, September 2007.

[5] C.S. Yim, A.K. Chopra, J. Penzien, Rocking response of rigid block to earthquakes. *Earthquake Engineering and Structural Dynamics*, **8**, 565-587, 1980.

[6] A.N. Kounadis, Parametric study in rocking instability of rigid block under harmonic ground pulse: A unified approach. *Soil Dynamics and Earthquake Engineering*, **45**, 125-143, 2013.

[7] I. Caliò, M. Marletta, Passive control of the seismic rocking response of art objects. *Engineering Structures*, **25**,1009-1018, 2003.

[8] A. Contento, A. Di Egidio, Investigations into the benefits of base isolation for non-symmetric rigid blocks. *Earthquake Engineering and Structural Dynamics*, **38**, 849-866, 2009.

[9] M.F. Dimentberg, Y.K. Lin, R. Zhang, Toppling of computer-type equipment under base excitation. *Journal of Engineering Mechanics*, **119**, 145-160, 1993.

[10] N. Makris, J. Zhang, Rocking response of anchored blocks under pulse-type motions. *Journal of Engineering Mechanics*, **127**, 484-493, 2001.

[11] Y.H. Chen, W.H. Liao, C.L. Lee, Y.P. Wang, Seismic isolation of viaduct piers by means of a rocking mechanism. *Earthquake Engineering and Structural Dynamics*, **35**, 713-736, 2006.

[12] H.Roh, A. M. Reinhorn, Nonlinear static analysis of structures with rocking columns. *Journal of Engineering Mechanics*, **136**, 532-542, 2010.

[13] L. Berto, T. Favaretto, A. Saetta, F. Antonelli, L. Lazzarini, Assessment of seismic vulnerability of art objects: The "Galleria dei prigioni" sculptures at the Accademia Gallery in Florence. Journal of Cultural Heritage, **13**, 7-21, 2012.

[14] H.W. Shenton, Criteria for initiation of slide, rock and slide-rock rigid-body modes. *Journal of Engineering Mechanics*, **122**, 690-693, 1996.

[15] A. Pompei, A. Scalia, M.A. Sumbatyan, Dynamics of rigid block due to horizontal ground motion. *Journal of Engineering Mechanics*, **124**, 713-717, 1998.

[16] S.C.S. Yim, H. Lin, Nonlinear impact and chaotic response of slender rocking objects, *Journal of Engineering Mechanics*, **117**, 2079-2100, 1991.

[17] F. Prieto, P.B. Lourenço, On the rocking behaviour of rigid objects. *Meccanica*, **40**, 121-133, 2005.

[18] S.C.S. Yim, A.K. Chopra, J. Penzien, Rocking response of rigid block to earthquakes. *Earthquake Engineering and Structural Dynamics*, **8**, 565-587, 1980.

[19] N. Makris, Y. Roussos, Rocking response and overturning of equipment under horizontal pulse-type motions. *Pacific Earthquake Engineering Research*, **5**, 1998.

[20] P.D. Spanos, A.S. Koh, Rocking of rigid block due to harmonic shaking, *Journal of Engineering Mechanics*, **110**, 1627-1642, 1984.